

A Theory of Dispersion Strengthening

F. V. LENEL and G. S. ANSELL

*Department of Metallurgical Engineering, Rensselaer Polytechnic Institute,
Troy, New York*

Abstract

Dispersion strengthening is explained by utilizing two methods of attack. The first, a theoretical approach, predicts the yielding and creep behavior of these alloys on the basis of dislocation theory. The second, an experimental approach, shows the variation of the yield and creep strength of these alloys with both the testing conditions and the structural parameters of these alloys.

The combination of these two approaches leads to a fundamental understanding of the mechanism involved in dispersion strengthening. In particular, requirements can be set as to the dispersion morphology required for achieving dispersion strengthening in an alloy system, based upon the fundamental constants of the alloy phases. These morphological requirements are applicable to dispersion-strengthened alloys in general. The additional requirement of high-temperature structural stability makes this treatment applicable to the S.A.P.-type alloys.

I. INTRODUCTION

A discussion of a theory of dispersion strengthening should properly begin with a definition of dispersion strengthening. When a finely divided second phase is distributed in a metallic matrix, an alloy is formed which is considerably stronger than the pure matrix metal by itself. This strengthening effect has long been recognized and made use of. Well-known examples are dispersions of cementite in a ferrite matrix, be it in the form of lamellar cementite in a pearlitic structure or of spheroidal cementite in tempered martensite structures. Leaving aside for the moment those precipitation-hardened alloys, in which the strengthening effect is attributed to the coherency strain between matrix and precipitate, there are many of these alloys which exhibit very marked dispersion-strengthening effects after coherency strains have been eliminated by overaging.

267

REPRODUCED BY
U.S. DEPARTMENT OF COMMERCE
NATIONAL TECHNICAL INFORMATION SERVICE
SPRINGFIELD, VA. 22161

N 52 12956

40

These dispersion-strengthened alloys by their very nature cannot be stable at elevated temperatures. They are produced by solid state reaction from alloys which are single phase at high enough temperatures; the finely dispersed second phase must, therefore, necessarily be soluble in the matrix. The second phase will have a tendency to reduce its surface area, even at temperatures below those where it dissolves completely. The dispersion will therefore become increasingly coarser with increasing times and temperatures. Since the hardening and strengthening effect of dispersion-hardened materials is strongly dependent upon the fineness of the dispersion, such coarsening will invariably cause a decrease in hardness and strength of the alloy.

The development of dispersion-strengthened alloys with a more stable phase at elevated temperatures has been primarily, although not exclusively, an accomplishment of powder metallurgy. This justifies a discussion of dispersion strengthening in this conference on powder metallurgy. The best known group of such alloys are the so-called "S.A.P. alloys," which consist of a dispersion of aluminum oxide in an aluminum matrix and are produced by compacting, hot pressing, and extruding aluminum flake or atomized aluminum powders.

A great deal of effort has been expended on developing dispersions of oxides in matrices other than aluminum, in the hope that these dispersions may be as stable up to the melting point of the matrix metal as the dispersions of aluminum oxide in aluminum are to the melting point of aluminum. Such oxide dispersions are produced by a number of methods. Finely divided metal powders and oxide powders may be mixed. Very thin oxide films may be deposited on the surface of metal powders or metal films on oxide particles. One of the oxides in a finely divided mixture of two or more oxides may be reduced to the metal and the resulting powder consolidated. Finally, internal oxidation of alloys, in which the solute metal forms a more stable oxide than the solvent metal and in which oxygen has appreciable solubility in the solvent metal, will lead to dispersions of a finely divided oxide in a metal matrix. The alloys may be internally oxidized as sheet or wire or in the form of powder which is subsequently consolidated by powder metallurgy methods.

The insoluble and stable second phase does not necessarily have to be an oxide. It may be an intermetallic compound such as the alu-

minum-zirconium intermetallic compound dispersed in a magnesium matrix which is precipitated when a mixture of magnesium-aluminum and magnesium-zirconium alloy powders is co-extruded.¹ Another example is an aluminum-iron intermetallic compound which is precipitated as a very fine dispersion in an aluminum matrix when a liquid aluminum-iron alloy is atomized.¹ This atomized powder can then be hot pressed and extruded without effect upon the fineness of the dispersion.

This listing indicates that there are a great many methods by which dispersion-strengthened alloys can be produced. However, this paper deals with the properties of these alloys and with the mechanisms by which these properties are achieved. The emphasis in this discussion will therefore not be on the methods of producing the alloys but upon their properties. The mechanical properties of an alloy are dependent only upon its microstructure and the interaction of dislocations with this microstructure and not upon the method of producing the alloy. Dispersion-strengthened alloys have several interesting properties. They have high yield strength; i.e., the stress necessary to cause incipient plastic deformation in the absence of any recovery process is high. They have a high rate of work hardening. Some of these alloys are quite ductile, i.e., their fracture stress is well above their yield stress; others are rather brittle, and ductility and brittleness depend strongly upon temperature. Dispersion-strengthened alloys with a more or less stable second phase have remarkably low creep rates at temperatures near the melting point of the matrix metal. They also strongly resist recovery and recrystallization when they are cold worked and annealed.

The theoretical treatment of strengthening in these alloys would be easy if all their properties could be explained by one mechanism. However, this is not possible. When one is interested in treating fundamentally the mechanical properties of an alloy, it is important not to treat a general characteristic of a material such as strength but rather the particular mechanical property which is of interest. Any mechanical property involving plasticity has to be evaluated in terms of dislocation motion. However, the mode of dislocation motion responsible for one particular property may not be important for another property; e.g., at low temperatures one is not concerned with dislocation climb, whereas at high temperature climb is necessary to explain recovery. Therefore it is not possible to propose a single

fundamental theory to explain all the mechanical properties of dispersion-strengthened alloys, but rather each mechanical property has to be treated individually. Several models have been suggested previously to account for the yield strength and flow stress of dispersion-strengthened materials. They have been applied to steels and to overaged precipitation-hardened alloys. These models appeared to be unable to explain the yield strength in the stable alloys of the S.A.P. type and a new model was, therefore, developed. If this model is correct, it should, of course, be valid for any dispersion-strengthened system which fits the model. In the first section of this paper, models previously suggested to explain the yielding and flow stress of dispersion-strengthened alloys are briefly reviewed, the new model for the yielding behavior of these alloys and the equations based on this model are presented, and some experimental data which support the new model are submitted.

One outstanding characteristic of the S.A.P.-type dispersion-strengthened alloys is their low creep rate. Considerable efforts have therefore been made to develop theories for the steady state creep behavior of these alloys and to correlate the theories with experimental data for creep. In the second part of this paper, dislocation models for steady state creep in dispersion-strengthened alloys are presented. Calculations for creep rate based on these models are developed and their results compared with experimental data for creep rate in several S.A.P.-type alloys.

For several other properties of dispersion-strengthened alloys no quantitative theory has yet been developed, notably their work-hardening behavior, their fracture properties, and their resistance to recovery when they are annealed. In a final section of this paper the directions are outlined which further theoretical and experimental work in this field should take.

II. THEORIES FOR YIELD AND FLOW STRESS OF DISPERSION-STRENGTHENED MATERIALS

Because of the great importance of precipitation strengthening in practical alloy development a great effort has been expended to further its understanding. An extensive review of dispersion-strengthened alloys formed by precipitation reactions was given by Geisler,² who attributed the major part of the strengthening to the

effects of coherency strains set up in the matrix by the precipitated particles with only a minor contribution due to the dispersed particles. It will become apparent in a later section that coherency strains are probably important because they change the effective dispersion morphology rather than create a different type of dispersion strengthening. Geisler's treatment of the problem therefore is more valuable as an adjunct to, rather than the basic strengthening mechanism for, dispersion-strengthened alloys.

Gensamer et al.,³ in order to account for the flow stress behavior observed in a series of steels, offered the following explanation for the strengthening effect of a dispersed second phase. The dispersed particles divide the material into blocks whose dimensions are equal to the interparticle spacing. These blocks then define the limit for the mean free path of dislocation motion. The number of dislocations moving over this mean dislocation path to produce a given strain is inversely proportional to the mean path. To produce strain at a certain rate, dislocations must be generated at a rate which is also inversely proportional to this path length. If the relation between the rate of formation of dislocations and the applied stress is known, then the effect of the mean dislocation path on the resistance to deformation at constant strain rate is also known. The relation between speed of deformation and stress is assumed to be semi-logarithmic, which appears to be the case for copper and steel at low temperatures. If the speed of deformation is proportional to the rate of generation of dislocations, then the stress should be proportional to the negative logarithm of the mean interparticle spacing. The formation of dislocations at a particular source is dependent only on the effective stress on the dislocation source. The effective stress on a dislocation source is the applied stress minus the back stress due to dislocation structure in the material. This back stress is the critical factor affecting the nucleation of dislocations.

Any theory purporting to explain deformation has to explain the effect of the change of dislocation structure by deformation on the variation of the back stress. In Gensamer's theory this area is side-stepped by assuming an arbitrary relationship between rate of deformation and rate of generation of dislocations from a source. This side-stepping of the actual deformation mechanism makes the theoretical explanation inadequate. The flow stress in many of the steels investigated by Gensamer was actually found to be inversely

proportional to the logarithm of the spacing, but this cannot be considered a proof of the theory. The relationship between dispersion spacing and flow stress which Gensamer established has later been extended to the relationship between dispersion spacing and yield strength.⁴ This extension is on even more uncertain footing, since there is no good theoretical reason to justify this extension. The fact that the data for yield strength of certain dispersion-strengthened alloys fit Gensamer's relationship must be considered fortuitous. Later a theory is proposed which fits the data as reasonably as does Gensamer's relationship.

Orowan^{5,6} has proposed that the critical shear stress of a dispersion-strengthened crystal should be proportional to the reciprocal of the mean spacing between dispersed particles. He suggests that as a dislocation approaches two dispersed particles it will bow out between them, finally connecting with itself beyond them, and leaving a residual dislocation loop surrounding each particle. The stress required to bow out the dislocation is inversely proportional to the radius of curvature assumed, and the maximum stress corresponds to the minimum radius of curvature through which the dislocation passes. This minimum radius of curvature is equal to half the distance between the particles. The critical shear stress is therefore inversely proportional to the spacing between dispersed particles. The model for dislocation movement in a dispersion-strengthened alloy appears to be correct. It will be shown, however, that in a large class of dispersion-strengthened materials, even when the stress is great enough to satisfy the Orowan requirement for yielding, macroscopically observable yielding has not yet occurred. According to the theory later developed in this paper, for actual yielding of dispersion-strengthened alloys it is necessary that the shear stress caused by the pile up of dislocations around or against the second phase particles increases to such an extent that the second phase particles are fractured or plastically deformed.

Fisher et al.⁷ have formulated a theory in which the contribution of dispersed particles to workhardening is calculated. The theory does not attempt to account for the yielding behavior of the dispersion-strengthened alloy, but assumes that the accumulation of residual dislocation loops surrounding the dispersed particles, due to the operation of the Orowan mechanism, gives rise to a back stress which must be overcome by dislocations subsequently moving on the

same slip planes as those on which the residual loops lie. This back stress is assumed to be a significant part of work hardening. The results of Fisher, Hart, and Pry's computations show that after a given amount of deformation, the shear stress for further deformation can be calculated. Fisher, Hart, and Pry's model can, of course, not be correct for any alloy for which the second phase particles must be sheared before macroscopic yielding has occurred. Once the particles are sheared, they cannot give rise to the formation of additional loops during work hardening.

III. DISLOCATION THEORY FOR YIELDING OF DISPERSION-STRENGTHENED ALLOYS

1. Introduction

Plastic deformation in crystals is due to the movement of dislocations. The crystals yield when large numbers of dislocations can move appreciable distances through the lattice. Dislocations are nucleated at sources in the lattice due to an applied stress. If the stress required to nucleate dislocations is greater than the stress necessary to move dislocations appreciable distances along a slip plane, the yield stress of the material will equal the stress necessary to nucleate the dislocations from a source. In alloys where a continuous three-dimensional dislocation network provides Frank-Read sources, this stress is equal to

$$\text{Nucleating stress} = \mu b/L \quad (1)$$

where μ is a shear modulus, b is the Burgers vector of the dislocation, and L is the linear distance between nodes of the dislocation network. For unresolved stresses and strains the right-hand side of this equation should be multiplied by 2.

In dispersion-strengthened alloys, however, the stress necessary to move dislocations appreciable distances along a slip plane may be higher than the stress necessary to nucleate dislocations from a source. In this case, the yield stress of the alloy is determined by the stress required to move dislocations freely in a crystal lattice containing a uniformly dispersed second phase. A model for calculating this stress follows.

2. Model

Dislocation loops are considered to be formed at dislocation sources under the action of an applied stress. The exact nature of the sources is not critical in considering the model. As the dislocation loops expand from the sources, they are either blocked from further motion by the dispersed second phase particles or they continue to move by bowing about the dispersed particles leaving residual loops surrounding each particle. The stress required to bow dislocation loops about the dispersed particles is the yield stress in the Orowan criterion for yielding,^{5,6} which predicts that the yield stress of dispersion-strengthened alloys is inversely proportional to the dispersed particle spacing. However, in this model it is postulated that even when the dislocations move past the dispersed particles, leaving residual dislocation loops surrounding the particles, yielding does not result. This postulate can be supported by the following argument.

The first dislocation nucleated at a source moves in the slip plane until it is blocked from further movement by its interaction with dislocations nucleated from other sources. In single phase materials this blockage of the lead dislocation is overcome by the increase of stress on the dislocation due to the pile up of subsequently nucleated dislocations behind the lead dislocation. In a dispersion-strengthened alloy, however, the lead dislocation remains blocked for the following reasons: (1) The stress field of the residual loops as in the Fisher et al.⁷ work-hardening model, decreases the effective stress on the dislocation source. Because the effective stress on the dislocation source is reduced, fewer dislocations are nucleated at each source. (2) The stress field of the residual loops interacts with the piled-up dislocation group changing the pile-up spacing. This reduces the stress field ahead of the leading dislocation of the piled-up group of dislocations. Both of these factors decrease the stress on the lead dislocation making it easier to be blocked. Therefore, the plastic strain ϵ of the dispersion-strengthened alloy is

$$\epsilon = MN\pi R^2b \quad (2)$$

where M is the density of dislocation sources, N is the number of dislocations nucleated at each source, R is the average radius of the dislocation loops, and b is the Burgers vector of the dislocations. Assuming reasonable values for these: $M = 10^9$ sources/cm³, $N = 10$

dislocations/source, $R = 1/2 (M^{-1/3})$, and $b = 2 \times 10^{-3}$ cm the resultant strain is about 10^{-4} . This is much less than the strain associated with yielding, e.g., the strain associated with the engineering offset yield stress of 2×10^{-3} . Therefore, plastic deformation stops and yielding has not occurred when the back stress on the dislocation source (due to an array of either blocked dislocations or of residual loops around the particles) exceeds the applied stress. The choice of the value for the source density in the evaluation of eq. (2) is not critical since the strain varies as the cube root of the source density. Under these conditions, in alloys with fine dispersions, no apparent yielding has yet occurred. In order to cause such yielding, the shear stress due to the dislocations piled up around or against the particles must fracture the dispersed second phase particles. This fracturing of the dispersed particles relieves the back stress on the dislocation source and also increases the stress on the lead dislocation. The dislocations then can sweep out areas on the slip plane which are large with respect to the dispersion spacing.

The fineness of a second phase dispersion necessary to make its fracture the critical requirement for yielding, depends upon the density of active dislocation sources in the alloy. The lower the dislocation source density, the coarser the dispersed particle spacing required to make the dispersed particle failure the requirement for yielding.

Even at one-half or more of the absolute melting temperature of the matrix metal, fracture of the second phase particles should be necessary for appreciable yielding unless recovery takes place. Recovery can occur either by climb of piled-up dislocations at a rate exceeding the applied strain rate or by cross slip of piled-up dislocations out of the slip plane if the geometry of the dispersed second phase particles permits. The possibility of recovery is not considered in the following calculation.

3. Calculations Based on the Model

On the basis of the preceding model, the yield strength of a dispersion-strengthened alloy is now evaluated. In this evaluation the shear stress on the dispersed particles due to dislocations piled up against or residual loops piled up around the particles is calculated for straight dislocation segments piled up against a straight barrier. This calculation is applicable to dispersion-strengthened alloys which contain dispersed particles of such a size and shape (e.g., flat plates

and large spheres) that the piled-up dislocations have a large radius of curvature and can be considered straight. This is the case for many of these alloys, e.g., S.A.P.-type alloys and most steels. In this case the stress τ on a dispersed second phase particle due to a piled up array of dislocations can be considered to be equal to

$$\tau = n\sigma \quad (3)$$

where n is the number of dislocation loops piled up against or around a dispersed particle and σ is the applied stress.

The number of dislocations n in eq. (3) acting on a particle depends upon the spacing between particles, according to:

$$n = 2\lambda\sigma/\mu b \quad (4)$$

where λ is the spacing between dispersed particles and μ is a shear modulus of the matrix metal [$\mu \approx \sqrt{1/2 C_{44}(C_{11} - C_{12})}$ for cubic metals, C_{ij} being the usual elastic constants]. Combining eqs. (3) and (4), the shear stress τ on the particle is equal to

$$\tau = 2\lambda\sigma^2/\mu b \quad (5)$$

The dispersion-strengthened alloy yields when the shear stress on the particle is equal to the fracture stress of the dispersed particle.

The limiting stress F that will fracture the dispersed particles is proportional to a shear modulus μ^* of the particle. Therefore

$$F = \mu^*/C \quad (6)$$

where C is a constant of proportionality, which can theoretically be shown to be somewhere in the neighborhood of 30.³

Combining eqs. (5) and (6) gives the maximum stress that can be applied to the alloy before yielding occurs. The yield stress of the alloy is therefore equal to

$$\text{Yield stress} = \sqrt{\mu b \mu^*/2\lambda C} \quad (7)$$

If the distribution of second phase particles is such that the stress calculated from eq. (7) is less than the stress necessary to cause dislocations to be nucleated from a source, the equation is no longer applicable. In this case, the yield stress of the alloy should be calculated from this dislocation-nucleating stress, which is the yield stress of the matrix metal without a dispersed second phase. If a continuous

three-dimensional network provides Frank-Read dislocation sources, this stress is given by eq. (1).

The calculation presented in this section is based on the assumption that the piled-up dislocations have a large radius of curvature and can be considered straight. When the radius of curvature is small, this calculation of the shear stress on the particles no longer holds. Instead, the treatment which Fisher et al.⁷ used to calculate the shear stress on a dispersed particle due to residual dislocation loops becomes applicable. In this treatment the stress on the dispersed particles due to residual dislocation loops is equal to

$$\tau = nb\mu/R \quad (8)$$

where R is the radius of a spherical dispersed particle. The minimum radius R_{\min} of the dispersed particles for which the treatment in this section is no longer applicable may be calculated by combining eqs. (3) and (8) and writing:

$$R_{\min} = b\mu/\sigma \quad (9)$$

This minimum radius is therefore dependent upon the particular alloy system in question and on the level of stress required to produce yielding. If for a particular alloy: $b = 10^{-8}$ cm, $\mu = 10^{11}$ dynes/cm², and $\sigma = 10^9$ dynes/cm², then R_{\min} is 10^{-6} cm. The two approaches (i.e., the one for particles larger and the one for particles smaller than R) are compatible with the model, each being the limiting case of the other. The model itself, which postulates shearing of the second phase particles is valid in either case, only the mathematical treatment must be varied to fit the appropriate case.

This model is based upon yielding occurring when the area swept out per dislocation loop is large as compared to the dispersed particle spacing. The particles act simply to hinder dislocation motion. The derivation is similar to that given by Petch,⁹ where grain boundaries are the blocking structure.

IV. REQUIREMENTS FOR DISPERSION-STRENGTHENED ALLOYS WITH HIGH YIELD STRENGTH

With the dislocation theory proposed for yielding, it should be possible to predict the yield strength of an alloy containing a finely dispersed second phase. However, in most of these alloys yield

strengths can be evaluated from eq. (7) only to an order of magnitude for two reasons: (1) The value of the constant of proportionality C in eq. (6) is very approximate since it depends upon what assumptions are made in its calculation, (2) The value of the shear modulus of the dispersed phase may not be known, or if it is known for the phase in bulk form, it may not be applicable to the fine particles in the dispersion because of differences in structure or composition. Nevertheless, it is interesting to note that by taking reasonable values for the shear moduli of dispersed phase and matrix the calculated yield strength of the alloys discussed below will fall within an order of magnitude of the experimental values.

Even though the dislocation theory does not yet permit calculation of absolute values of yield strength of dispersion-strengthened alloys, it will furnish a guide for the design of these alloys. The theory predicts the variation of yield strength with the degree of dispersion in these alloys. It shows how the nature of the matrix metal and of the second phase influence the strength of the alloy. For certain systems it predicts how the yield strength of an alloy varies with temperature. The theory will also indicate whether the yield strength of a given alloy consisting of particles of a second phase dispersed in a matrix is due to the dispersion-strengthening mechanism or not. Finally, the theory will answer questions regarding the nature of the dispersed particle-matrix interface. Experimental data are available to test the predictions of the theory with regard to the relationships between yield strength and particle spacing, between yield strength and the nature of the phases involved, and between yield strength and temperature in a given system. These data are presented in the following sections. They are followed by qualitative discussions of the range of validity of the dispersion-strengthening mechanism and of the requirements for dispersed phase-matrix interfaces in dispersion-strengthened alloys.

1. Effect of Dispersion Spacing upon Yield Strength

According to eq. (7) the yield strength of a dispersion-strengthened alloy should vary linearly with the reciprocal of the square root of the dispersion spacing. The line should extrapolate to zero for dispersions with an infinite spacing. In order to verify this relation, data are necessary on the spacing of the second phase in these alloys and their yield strengths. The yield strength predicted by the theory is

the stress required to produce apparent yield in the alloy. In single crystals this stress can be identified with the critical resolved shear stress. In polycrystalline material, a yield strength may be used with an offset corresponding to the strain at which the second phase particles fracture. As indicated in the theory section this strain will in most cases be considerably less than the 0.2% offset used for the

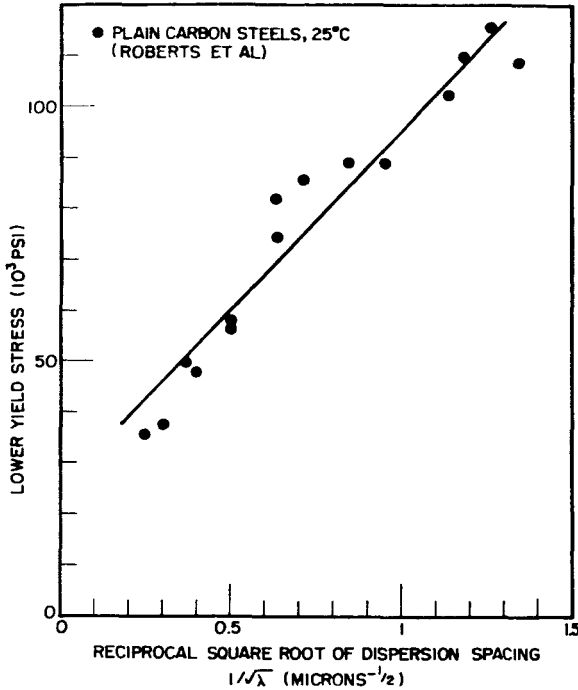


Fig. 1. The lower yield points of several hypoeutectoid, eutectoid, and hypereutectoid steels are plotted vs the reciprocal square root of dispersion spacing. The line represents the least squares fit of the data.

engineering yield strength. The assumption may be made that for a given series of alloys tested at constant temperature the engineering 0.2% offset yield strength is a constant amount higher than the yield strength postulated by the theory. In that case the engineering yield strength should also be proportional to the reciprocal of the square root of the spacing, but the intercept of the straight line

between yield strength and reciprocal of the square root of spacing should have a positive intercept at infinite dispersion spacing. Roberts et al.⁴ determined the lower yield strength of several hypoeutectoid, eutectoid, and hypereutectoid steels, some with a pearlitic and others with a spheroidized structure. In a few cases the elastic limit was also measured. For this same series of steels, the authors de-

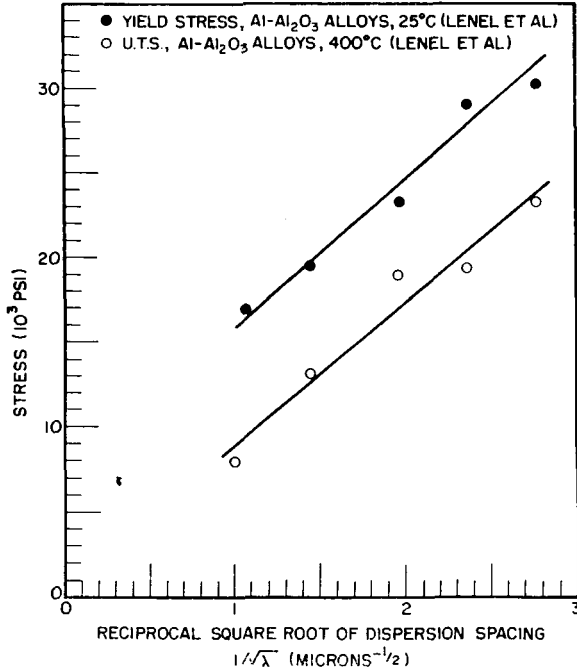


Fig. 2. The room temperature yield strengths and the ultimate tensile strengths at 400°C for several Al-Al₂O₃ S.A.P.-type alloys are plotted vs the reciprocal square root of the dispersion spacing. Each line represents the least squares fit of the data.

termined the mean ferrite path, which they defined as the mean distance between carbide particles or pearlite patches. They plotted the lower yield point, and where available the elastic limit, versus the logarithm of the mean free path. This relationship, which was first proposed by Gensamer et al.³ for flow stress must be considered empirical as is discussed in the Introduction. In accordance with the theory proposed here, the lower yield points of Roberts et al.⁴

were replotted in Figure 1 versus the reciprocal of the square root of the spacings. A least squares line has been drawn assuming a linear relationship. The fit is as satisfactory as that shown in the original plot of Roberts et al. Unfortunately, too few values were available for establishing a valid correlation between elastic limit and spacing.

Lenel, Ansell, and Nelson¹⁰ determined by quantitative electron microscopy the average spacing between the plate-like oxide particles, for a series of flake aluminum powder extrusions of the S.A.P. type. For these same extrusions, Lenel, Backensto, and Rose¹¹ determined the room temperature yield strength at 0.2% offset and the ultimate tensile strength at 400°C. At 400°C, the ultimate tensile strength and the tensile yield strength are almost equal.¹² In Figure 2, the strength values at the two temperatures are again plotted versus the reciprocal of the average spacing, with the lines representing the least squares fit of the data. This plot does not exhibit any more scatter than the empirical type of plot suggested by Lenel for his data.

The critical resolved shear stress of a series of overaged high-purity aluminum-copper alloys and the spacing between the dispersed second phase particles in these alloys were determined by Dew-Hughes and Robertson.¹³ They interpreted the data as supporting Orowan's yield strength theory. A least squares analysis of the data plotted according to Orowan's theory, however, shows neither predicted linear variation of the critical resolved shear stress with the reciprocal of the dispersion spacing, nor a line intercept of zero for an alloy with an infinite spacing. On the other hand, if their values for the critical resolved shear stress are plotted versus the reciprocal of the square root of the dispersion spacing as is shown in Figure 3, a better fit is obtained. The line represents the least squares fit of the data and goes through the origin of the graph. This indicates that the proposed theory, in which yielding takes place when the dispersed second-phase particles shear, would also apply to aluminum alloys containing a dispersion of the theta phase. Dew-Hughes and Robertson consider this possibility, but conclude from an examination of the micrograph of a fractured sample near its fracture surface that the particles do not shear during plastic deformation of the matrix. However, it appears doubtful that the shear of the particles as proposed in this paper can actually be detected by this type of examination.

2. Effect of Alloy System upon Yield Strength

The dislocation theory indicates that the yield strength of a dispersion-strengthened alloy depends upon the strength of both the matrix and the dispersed phase. Only alloys in which the second phase is stronger than the matrix will exhibit dispersion strengthening. The theory permits an evaluation of the effect of a particular metal matrix-dispersed phase combination used in fabricating a dispersion-strengthened alloy. According to eq. (7) the larger the value of the shear modulus of the dispersed second phase, the steeper should be the slope of the curve of yield strength versus the reciprocal of the square root of the dispersion spacing. This is shown to be true in comparing the slope of the lines representing the least squares fit of the data in Figures 2 and 3. In both cases the matrix metal of the alloy is alu-

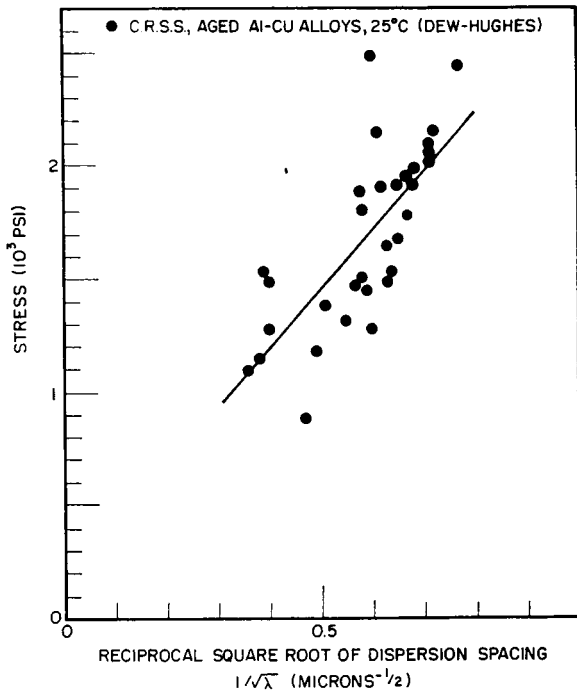


Fig. 3. The critical resolved shear stress of several overaged Al-Cu alloys are plotted vs the reciprocal square root of the dispersion spacing. The line represents the least squares fit of the data.

minum, but the alloy whose yield strength data are shown in Figure 2 has aluminum oxide as the dispersed second phase as compared to the copper-aluminum theta phase for the alloy represented in Figure 3. The shear modulus of the oxide is approximately 10 times greater than that of the theta phase. The ratio of the slopes of the two lines should therefore be equal to $\sqrt{10}$, if the mode of failure of these two dispersed phases is similar and the constant of proportionality C in eq. (6) the same for the two alloys. The actual ratio of the slopes of the two lines is 3, in good agreement with the theory.

3. Temperature Dependence of the Yield Strength

Inspection of eq. (7) shows that of the terms which determine the yield strength of a dispersion-strengthened alloy, only the shear moduli have an appreciable temperature dependence. Therefore, if the temperature dependence of these moduli is known, or if a reasonable approximation of this dependence can be made, the variation of the yield strength with temperature should be predictable according to the equation

$$\sigma_T = \sigma_{25}(\mu_T\mu_T^*/\mu_{25}\mu_{25}^*)^{1/2} \quad (10)$$

in which σ is the yield stress, and μ and μ^* the shear moduli of the matrix metal and the dispersed phase, respectively; the subscripts refer to the values of the properties at test temperature and at 25°C.

This predicted temperature dependence can be checked by determining the temperature dependence of the proportional limit, assuming that the proportional limit in these alloys is the stress which causes the second phase particles to shear. The temperature dependence of the proportional limit of two aluminum-aluminum oxide S.A.P.-type alloys, MD 2100 and MD 5100, has been determined recently by Lenel, Ansell, and Bosch.¹⁴ The proportional limit was determined by sensitively measuring the strain in these materials as a function of stress. In Figure 4 the values of stress divided by strain are plotted as a function of strain for one particular test. This type of plot unambiguously shows the first deviation from the linear stress-strain relationship permitting an accurate determination of the proportional limit. For both of these alloys, the proportional limit was determined over the temperature range from 0.1 to 0.87 homologous temperature (90–773°K) and the yield strength (0.2% offset) in the

range from 0.1 to 0.6 homologous temperature (90–530°K). The data are plotted in Figure 5. In the same figure, lines are plotted of the temperature dependence of the proportional limit according to eq. (10). The data for the shear modulus of aluminum as a function of temperature were interpolated from the data of Sutton¹⁵ for the elastic constants of high purity aluminum. The data for the shear modulus of aluminum oxide were interpolated from the data of Stavrolakis and Norton¹⁶ for the modulus of rigidity of compacted and sin-

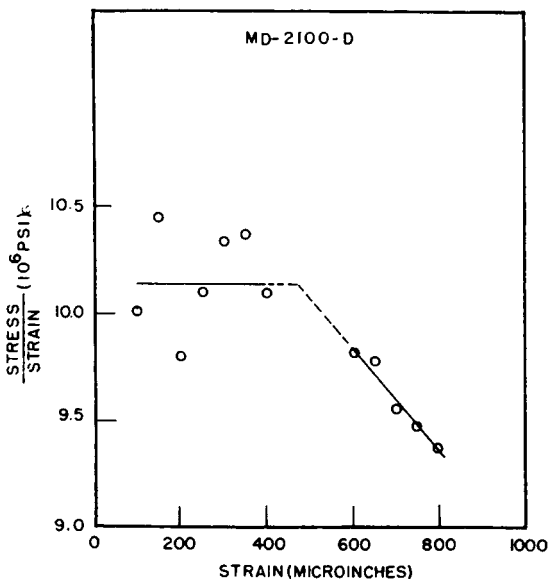


Fig. 4. The ratio of stress divided by strain on an Al-Al₂O₃ S.A.P.-type alloy is plotted as a function of strain to determine the proportional limit.

tered alumina. The data for aluminum are quite extensive and can be considered reliable in this temperature range. Very little reliance can be placed in the data for the aluminum oxide, however, because of the few data determined in this temperature range. In view of the uncertainty of the modulus data for aluminum oxide, the agreement between the theoretically calculated and the experimentally determined proportional limit-temperature relationship may be considered reasonable. It is certainly much better than for the experimental 0.2% offset yield strength curve.

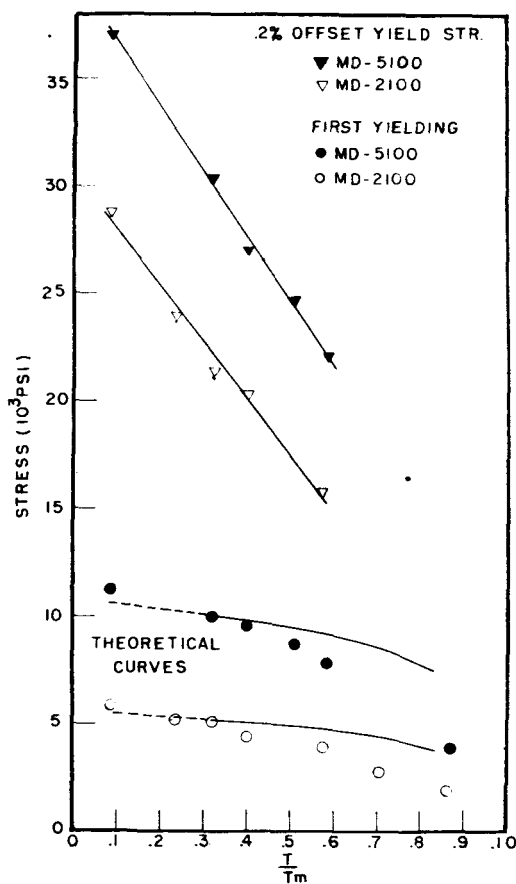


Fig. 5. The offset yield stress and proportional limit of two Al-Al₂O₃ S.A.P.-type alloys are plotted as a function of temperature. Lines are shown giving the temperature dependence of the proportional limit predicted by eq. (10).

4. Cold-Worked and Dispersion-Strengthened Alloys

In discussing the theory of dispersion strengthening, Grant¹⁷ has placed emphasis upon the effect of "stored energy," which is derived from cold working the alloy. Cold work strengthens a single phase alloy by increasing the dislocation density and, at least in the case of face-centered cubic metals, by forming Cottrell-Lomer barriers. Dispersion-strengthened alloys may be strengthened by

cold work in a similar way. However, this strengthening effect is not lost as readily in these alloys because of their resistance to recovery, as will be discussed in the section on creep theory in this paper. The problem arises: What are the relative contributions of the stored energy effect on the one hand and the stress necessary to shear

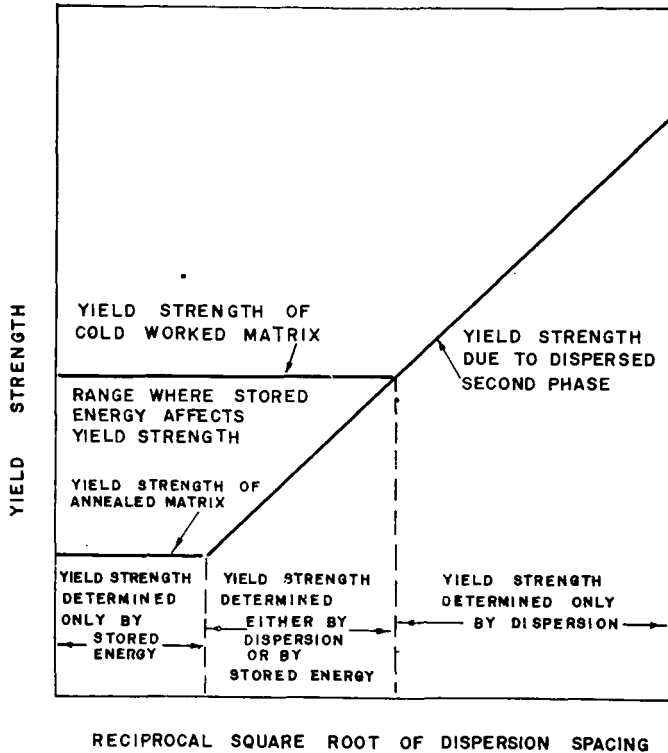


Fig. 6. A schematic graph of the relative effects of dispersion spacing and stored energy upon the yield strength of dispersion-strengthened alloys.

second phase particles on the other hand to the increased yield strength of dispersion-strengthened alloys?

One may consider the problem in the following manner: The stored energy causes an increase in the yield strength of the matrix metal. By cold working, the density of dislocations is increased, and therefore the length of Frank-Read sources present in the matrix

decreased. This in turn raises the stress to nucleate dislocations as given in eq. (1). If this stress to nucleate dislocations is greater than the stress required to cause dislocations to fracture the second phase particles, then the yield stress of the dispersion-strengthened alloy is determined by the amount of stored energy. If the nucleating stress is less, then stored energy has no effect on the yield strength of dispersion-strengthened alloys. This is shown in Figure 6 where, for dispersed particle spacings which are very large, the strength of the alloy is the strength of the matrix metal. For intermediate spacings, the yield strength is determined either by the dispersion or stored energy, whichever is greater. For very fine dispersion spacings the yield strength is not affected by stored energy but is determined by the dispersion. How fine a dispersion must be so that an alloy falls into the third category will depend upon the shear moduli of the matrix metal and the dispersed second phase at the temperature in question because the strengthening mechanism is a function of both of them.

5. Dispersed Particle-Matrix Interface

The theory proposed for the strengthening of a metal by the addition of a dispersed second phase depends upon the dispersed phase impeding the movement of dislocations. For this purpose the interface between the dispersed phase and the metal matrix cannot act as a free surface. A dislocation in a crystal lattice has a strain field associated with it. On approaching a free surface, the strain field on the surface side of the dislocation is relaxed as compared with the strain field of the dislocation facing the interior of the crystal. This net unbalance of the dislocation strain field acts to move the dislocation toward the free surface and it eventually runs out of the crystal. If, instead of a free surface, the surface of the crystal is elastically stronger than the crystal lattice, then the unbalance of the strain field is of the opposite sign to the preceding case for a free surface; i.e., the dislocation will be repelled from the surface. In dispersion-strengthened alloys, for the particles to hinder dislocation movement, the dislocations have to be repelled from the dispersed phase-matrix interface. Therefore the interface has to be of such a nature that the strain field of the dislocation can be transmitted from the matrix lattice, through the interface, into the lattice of the dispersed phase. In order to accomplish this the matrix has to "wet," adhere to, or cohere with

the dispersed particles. This characteristic of the effects of free surfaces and of adherent coatings on surfaces has been clearly shown by Barrett¹⁸ in his experimental investigations of the elastic aftereffect for wires twisted in torsion. A similar investigation of the presence or absence of the elastic aftereffect in wires of the matrix metal coated with a proposed dispersed phase should give a good indication of whether the interface between the two phases of a particular two phase system possesses this required property.

This discussion brings out the fact that in order to obtain dispersion strengthening the second phase may cohere but does not have to cohere to the matrix. The principal characteristic of the coherency effect is the lattice strain it produces in both the matrix and the second phase. The range of these coherency strains may be of the order of the dispersed particle spacing. For the purpose of calculating dispersion-strengthening effects, the size of a complex consisting of the precipitated particle and the strained coherent region of the matrix surrounding it should be important, rather than the size of the particle alone. When precipitation hardening is considered from this point of view, the small spacing between these complexes would furnish the major contribution to the high yield strength of precipitation-hardened alloys.

V. DISLOCATION THEORY AND EXPERIMENTAL DATA FOR CREEP

1. Introduction

Creep is the extension of crystals under constant stress at a constant temperature. Creep behavior has been described rheologically for many years. Not all the different modes of creep which have been observed can be readily explained on the basis of a dislocation model. However, one type of creep lends itself well to such a treatment. This is steady state creep, i.e., creep at a constant rate, at temperatures above one-half of the absolute melting temperature.

In order to treat steady state creep, models must be set up for the metallurgical structure and the dislocation array of the alloy and the assumption made that both structure and array remain constant. The rate is then evaluated by calculating the density of dislocations moving in the crystal and their rate of motion. Two creep theories have been developed by Ansell and Weertman¹⁹ for dispersion-

strengthened alloys of the S.A.P. type. The first theory should be applicable to alloys in which the area-to-volume ratio of grain boundary of the alloy is small. Such coarse-grained dispersion-strengthened alloys with grain diameters of several millimeters may be produced by cold working and then recrystallizing aluminum powder extrusions.²⁰ Ansell and Weertman base their theory for the creep of these coarse-grained alloys on a model for creep essentially due to Mott and adopted by Weertman.^{21,22} According to this model, dislocation loops are created at sources under the action of an applied stress. The loops expand to some maximum radius at which point they are annihilated by climbing to dislocations of opposite sign on neighboring slip planes. Just as fast as loops are destroyed, new loops are created at the sources and steady state creep is produced. For single phase material the rate-controlling process for creep can be either the climb of dislocations²¹ or the viscous motion of a dislocation by some microcreep mechanism.²² For coarse-grained dispersion-strengthened alloys it is reasonable to assume, as suggested by Schoeck,²³ that the rate-controlling process for steady state creep is the climb of dislocations over the second phase particles.

Ansell and Weertman's second creep theory was developed to account for the creep behavior of fine-grained dispersion-strengthened alloys of the S.A.P. type. It applied to aluminum powder extrusions in the as-extruded condition which have needle-like grains approximately 5μ thick. For these materials the activation energy for steady state creep is abnormally large. This was explained by Ansell and Weertman by assuming that dislocations nucleated at the grain boundaries are primarily responsible for the creep deformation while dislocations nucleated from active dislocation sources of the type found in the coarse-grained alloys contribute much less to creep.

In the following sections each of the two theories is presented together with the experimental data supporting it.

2. Steady-State Creep Defined by Dislocation Climb

In order to calculate steady state creep rates based on dislocation climb somewhat different models have to be adopted for a low stress region, in which the stress is insufficient to bow dislocation loops about the particles, and for a high stress region, in which the stress will cause bowing of the loops. For both models an assumption must be made concerning the origin of the dislocations in the dispersion-

strengthened matrix. These dislocations must be nucleated from a constant set of dislocation sources present in the alloy. In order to calculate creep rates, Ansell and Weertman assumed that the density of sources would be approximately the same as in a well-annealed pure metal. The first attempts to compare calculated steady state creep rates with those determined in creep experiments were made on recrystallized MD 2100 alloy having a spacing between oxide particles of approximately 0.5μ . These attempts were unsuccessful, since the experimental creep rates were so low (less than $10^{-8}/\text{min}$) that they could not be determined. Later on, creep experiments were made on recrystallized aluminum powder extrusions with coarser spacings between oxide particles. For these alloys the steady state creep rate in the low stress region was still too low to be measured. However, in the high stress region, steady state creep could readily be determined. The dependence of these creep rates on stress, on temperature, and on the microstructure of the alloys showed that the Ansell-Weertman theory was on firm ground, even though the absolute values of the creep rate were several orders of magnitude lower than those calculated on the assumption of a dislocation source density similar to that in annealed metals.

(a) *Theory at Low Stresses*

First the creep rate is calculated in the stress range from a stress which would be just sufficient to activate a dislocation source, up to a stress which is great enough to force a dislocation past the particles by bowing dislocation loops about the particles. In this stress range dislocations do not pile up, because if the stress is great enough to pile up dislocations it is great enough to bow them past the particles. At low temperatures no plastic deformation takes place in this stress range because the dislocations cannot be moved past the particles. At high temperatures, however, plastic deformation can take place as the dislocations can climb around the particles.

In order to make the calculations it is necessary to use a number of parameters which are best described by means of diagrams. Figure 7a pictures a dislocation source imbedded in a field of second phase particles. The plane of the paper is the slip plane. Figure 7b shows a cross-sectional view of dislocation loops some time after the application of a stress. The slip plane is horizontal and perpendicular to the plane of the paper. Figure 7c shows a view of a length of dis-

location line looking down the direction of motion of the dislocation. The slip plane is again horizontal and perpendicular to the plane of the paper. Figure 7c illustrates the fact that it is equally probable that a segment of dislocation line may climb either over or under a particle. In one direction of climb vacancies (or interstitials) must be absorbed by an edge-type dislocation and in the other direction they must be released.

The creep rate may be calculated from the model shown in Figure 7 in the following manner. The creep rate is equal to the product of the number of dislocation sources per unit volume giving off disloca-

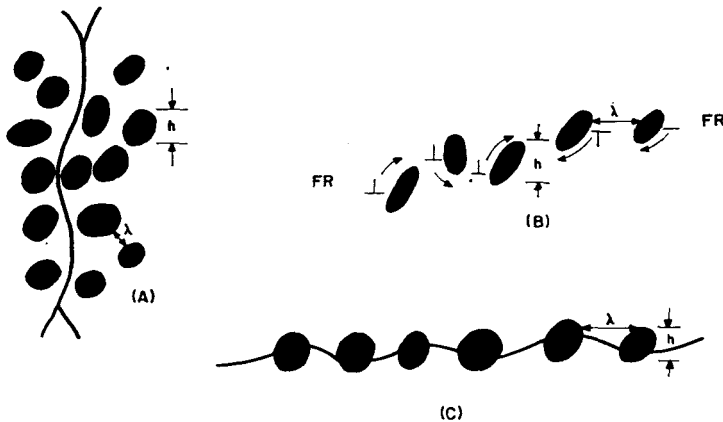


Fig. 7. Dislocation motion during steady state creep at low stresses: (a) dislocation source with slip plane in plane of paper, (b) dislocation loops under stress with slip plane horizontal, (c) dislocation line viewed from the direction of motion.

tion loops, the plastic strain produced by one dislocation loop upon expansion to its maximum radius, and the rate of production of dislocation loops at any one source. The creep rate K is therefore equal to

$$K = M\pi\mathcal{L}^2bR \quad (11)$$

where M is the density of dislocation sources, \mathcal{L} is the maximum radius, b is the length of the Burgers vector of a dislocation, and R is the rate of creation of dislocations at one source.

The maximum radius \mathcal{L} can be calculated from the following argu-

ment.^{21,22} The probability must be essentially one that at the maximum radius \mathcal{L} a dislocation loop is blocked from further expansion by dislocations on neighboring slip planes. Consider a pill box of radius \mathcal{L} and height d . Let one dislocation source be situated at the center of this pill box. There must be three other dislocation sources in the box since it takes at least three other sources to block a dislocation loop.²⁴ These conditions mean that the value of \mathcal{L} must be such that

$$2M\pi\mathcal{L}^2d \approx 3 \quad (12)$$

or

$$\mathcal{L} = \sqrt{1/2Md} \quad (13)$$

where d is the distance climbed by a dislocation in order to annihilate a dislocation on a neighboring slip plane. In the calculation of the steady state creep rate of a single phase alloy^{21,22} the distance d is a function of stress. In the present problem the distance of climb around particles is fixed by the geometry of the dispersed phase (distances of the order of a micron), and is usually greater than the stress-dependent values of d for single phase alloys. Thus it is reasonable in the present calculations to take a stress-independent value of d equal to the dimensions of the particles ($d = h$).

Consider next the term R , the rate of creation of dislocation loops, which appears in eq. (11). This rate is equal to the rate at which dislocations surmount barriers in Figure 7b. This is equal to the height of climb divided by the velocity of climb:

$$R = v/h \quad (14)$$

This velocity of climb is controlled by the diffusion of vacancies or interstitials. Weertman²⁵ calculated the velocity of climb for a dislocation which could maintain an equilibrium concentration of vacancies in its vicinity. This velocity was

$$v \approx \sigma b^2 D / kT \quad (15)$$

where σ is the stress, D is the coefficient of self-diffusion, k is Boltzmann's constant, and T is absolute temperature. The equation is valid for an edge dislocation which is climbing by itself some distance away from other dislocations.

Combining eqs. (11), (13), and (15) gives for the creep rate

$$K = \pi \sigma b^3 D / 2kT h^2 \quad (16)$$

(For unresolved stress and strain rates the right-hand side of this equation should be divided by $2\sqrt{2}$).

(b) *Theory at High Stresses*

Now an expression for the creep rate will be developed for stresses great enough for dislocations to be forced past the particles by bowing about the particles leaving residual dislocation loops surrounding and piled up against each particle. The process is shown in Figure 8.

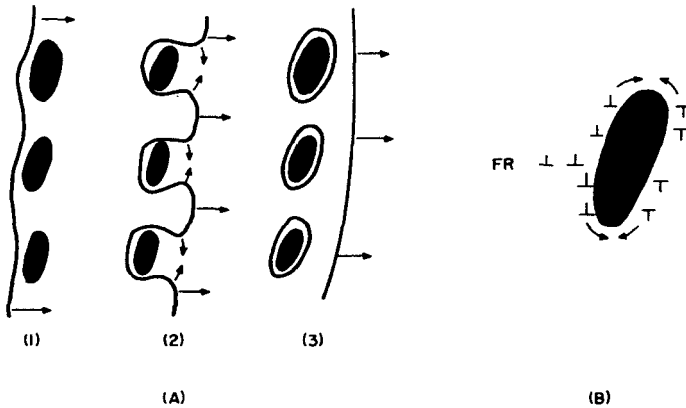


Fig. 8. Dislocation motion during steady state creep at high stresses: (a) pinching-off of dislocation loops and (b) climb of loops around dispersed particle.

The rate-controlling process now is the climb of the residual dislocation loops around the particles as shown in Figure 8b. The climb of these loops will be governed by the diffusion of vacancies away from or toward a dislocation line. Since the interface between the metal matrix and the included particle should be a good source or sink of vacancies, the vacancy flow will probably be between this interface and the dislocation lines.

The rate at which the residual dislocation loops are annihilated in Figure 8b may be estimated. The loops are forced to climb around the particles because of the interaction forces of the dislocations piled

up against the particles. The number n piled up in the distance λ , the dispersion spacing, is

$$n \approx 2\sigma\lambda/b\mu \quad (17)$$

The distance a residual dislocation loop must climb before another loop can be pinched off about the particle is of the order

$$\Lambda \approx \mu b/n\sigma \approx \mu^2 b^2 / 2\sigma^2 \quad (18)$$

The rate of climb of the dislocation loop is given by eq. (15) with the stress replaced by the concentrated stress $n\sigma$ or

$$v = 2\sigma^2 b \lambda D / \mu k T \quad (19)$$

R , the rate of dislocation nucleation, is equal to the dislocation velocity v divided by the height of climb Λ . Combining eqs. (18) and (19) yields the expression

$$R = 4\sigma^4 \lambda^2 D / b \mu^3 k T \quad (20)$$

Using the same argument for the dislocation source density as related to the maximum radius of expansion of dislocation loops as for the low stress case, eqs. (11), (13), and (20) are combined. This gives for the creep rate

$$K = 2\pi\sigma^4 \lambda^2 D / h \mu^3 k T \quad (21)$$

which is valid up to stresses where $n\sigma b^3/kt$ becomes greater than one. If unresolved stresses and strain rate are used, the right-hand side of this equation should be divided by $16\sqrt{2}$.

At stresses great enough that $n\sigma b^3/kT$ is greater than one, the velocity is no longer given by eq. (19) but is now^{21,25}

$$v = (D/2b) \exp\{n\sigma b^3/kT\} \quad (22)$$

The creep rate then becomes

$$K = (\pi\sigma^2 \lambda D / \mu^2 b^2 h) \exp\{2\sigma^2 \lambda b^2 / \mu k T\} \quad (23)$$

One must assume, of course, in the application of eq. (23) that the included particles are strong enough to withstand the stresses exerted by the dislocations piled up against them. In the stress range where eq. (23) is valid these stresses are very large and the particles may fracture or plastically deform. If the particles do yield, eq. (23) may merely set a lower limit to the creep rate.

(c) *Creep Data for Coarse-Grained Recrystallized Alloys*

Steady state creep data for three coarse-grained recrystallized alloys produced from aluminum powder have been obtained. The alloys consist of a fine dispersion of aluminum oxide platelets in a matrix of commercially pure aluminum. The oxide platelets are approximately 130 Å thick and 0.3μ on edge. The alloys designated MD 2100,²⁰ AT 400, and RP 15-30 were fabricated by compacting, hot pressing, and then hot extruding three types of aluminum powder:

- For MD 2100: A flake powder with an average flake thickness of 0.9μ .
- For AT 400: An atomized powder with 3μ average diameter particles.
- For RP 15-30: An atomized powder having a particle size range between 15 and 30μ .

The average dispersion spacing is approximately 0.5μ for the MD 2100 alloy, 1μ for the AT 400 alloy, and 6μ for the RP 15-30 alloy. After the initial fabrication process, the alloys were heavily cold worked by wire drawing and then annealed. The recrystallized alloys had a grain size of several millimeters.¹⁹

Samples of these recrystallized alloys were creep tested under the condition of constant loading. Since the creep strains were small the tests can be considered constant stress tests. The steady state creep rates obtained for all these alloys were several orders of magnitude slower than would be predicted from the creep theory based upon dislocation climb.

The steady state creep rate of the recrystallized MD 2100 alloy was slower than the sensitivity of the creep test apparatus, 10^{-8} min^{-1} for all temperatures up to 600°C and stresses as high as $3.5 \times 10^8 \text{ dynes/cm}^2$. Therefore, these data shed little light on the creep theory.

The steady state creep rates of the AT 400 and RP 15-30 recrystallized alloys were fast enough to be measurable in the high stress region as shown in Figure 9. In this figure the steady state creep rates for the two alloys at 500°C are shown on a logarithmic scale as a function of stress along with creep rates predicted by the creep theory at 500°C and the creep rate of high purity aluminum at 483°C . Although the absolute value of the creep rates is much lower for the AT

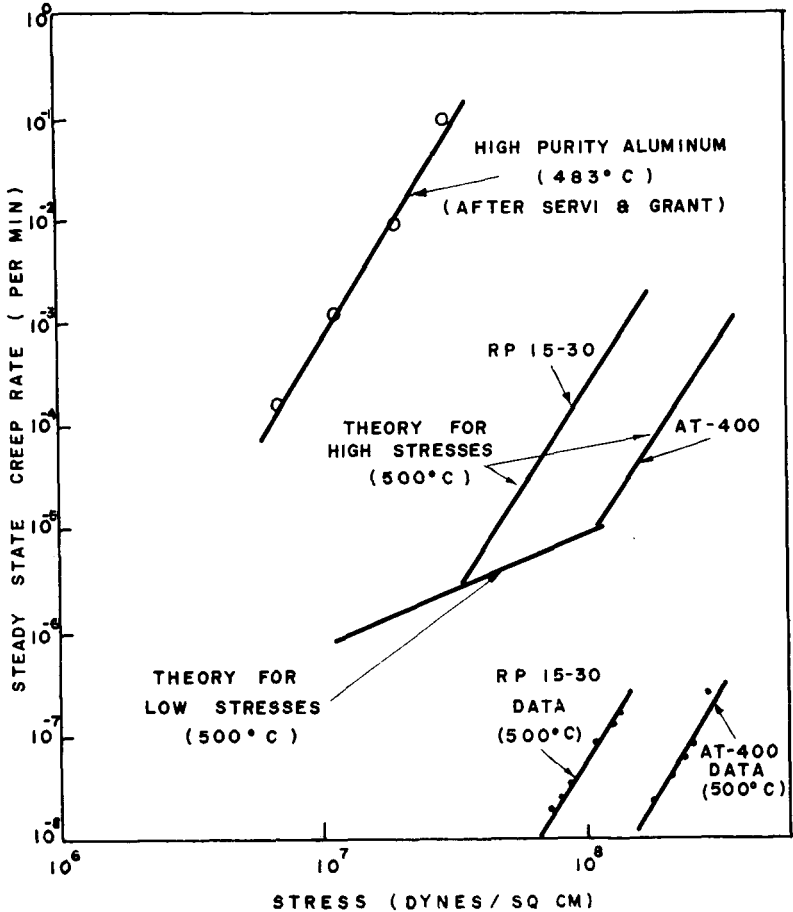


Fig. 9. The logarithm of the steady state creep rates of AT 400 and RP 15-30 recrystallized Al-Al₂O₃ S.A.P.-type alloys at 500°C and pure aluminum at 483°C are plotted vs the logarithm of the applied stress. Lines are drawn representing the steady state creep rates of the AT 400 and RP 15-30 alloys predicted by eq. (21).

400 and RP 15-30 alloys than would be predicted by the theory, there are two factors shown in the figure predicted by the theory. First the steady state creep rate of these alloys at high stresses varies as predicted, as the fourth power of the applied stress. Secondly, the creep rates in this stress range are proportional to the

square of the dispersion spacing. The creep rate of the RP 15-30 is about 32 times faster than the rate of the AT 400 alloy, while their respective dispersion spacings are at a ratio of 6 to 1.

For the AT 400 recrystallized alloy, creep rates at several temperatures have been determined. To compare these data with each other the creep rates were compensated to a single temperature by eliminating temperature as a variable in eq. (21). For this purpose only those terms in the equation which are temperature dependent (i.e., μ , D , and T) must be considered. To take the temperature dependence of the self-diffusivity D into account, it is expanded into the term $D_0 \exp\{-Q/RT\}$. The temperature-compensated creep rate K^* can then be written:

$$K^* = K(\exp\{-Q/R\theta\})/\{-Q/RT\})(\mu_T/\mu_\theta)^3(T/\theta) \quad (24)$$

in which T and θ are test temperature and reference temperature respectively, and the subscripts T and θ refer to the properties at these temperatures. In order to calculate temperature-compensated creep rates, the value of the activation energy Q must be known. This value was determined experimentally by conducting creep tests in which the stress was held constant and the temperature suddenly changed. At each of these temperatures creep rates were observed after they had assumed a steady state value. Using eq. (21), a value for Q of 37,000 cal/mole was determined from the creep rates at the two temperatures. This is in good agreement with the activation energy for self-diffusion in aluminum, indicating that dislocation climb is the rate-controlling process for steady state creep in this alloy.

In Figure 10 the logarithm of the steady state creep rate of the AT 400 alloy compensated to 500°C is plotted versus the logarithm of the applied stress. Using temperature compensation, creep over a much wider range of stresses can be plotted than for single temperature creep as in Figure 9. The slope of the straight line in Figure 10 was drawn to correspond to a fourth power stress dependence of the steady state creep rate. The position of the line was arbitrarily taken to fit the data. The agreement of the data points with the fourth power line again indicates that for the high stress region the data are in agreement with the creep theory. On the other hand, it is seen that for stresses lower than a certain value the creep rate falls rapidly to

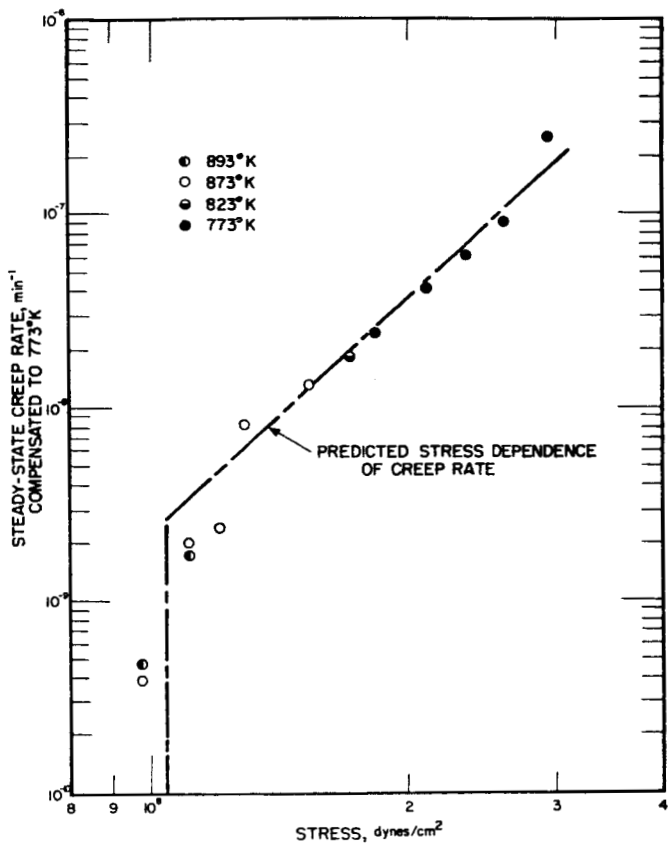


Fig. 10. The logarithm of the temperature-compensated steady state creep rate of the recrystallized AT 400 Al-Al₂O₃ S.A.P.-type alloy vs the logarithm of the applied stress.

very low values instead of following the first power relationship predicted by the theory for low stress.

(d) Dislocation Sources

The experiments indicate that the steady state creep rates for coarse-grained dispersion-strengthened alloys are much lower than those calculated on the assumption of active dislocation sources due to a continuous three-dimensional dislocation network. This leads

to the conclusion that the normal number of dislocation sources in these alloys is much reduced compared to that found in single phase metals. Ansell²⁶ suggested that this is due to the interaction of the dispersed particles with the dislocation network, either inactivating many of the sources or preventing network formation entirely. If such is the case, other types of dislocation sources must be the only active sources present in the alloy. These sources may be Frank-Read sources due to short dislocation segments running between particles, grain boundaries, or some type of lattice imperfections.

3. Steady-State Creep Defined by Dislocation Nucleation from Grain Boundaries

(a) Theory

In the case where the normal types of dislocation sources in the alloy are not active, dislocations may be nucleated from other imperfections in the structure, for example, at grain boundaries. This type of steady state creep behavior cannot be quantitatively evaluated but may be explained qualitatively in the following way.

With the aid of applied stress and thermal stress fluctuations, dislocations pop out of a grain boundary and move across the grain and join another grain boundary. The rate-controlling process for steady state creep is this "popping" out of the dislocation from the boundary. The energy required for this process is undoubtedly stress dependent and decreases with increasing stress. Let it be written as $Q(\sigma)$. Then in any narrow stress range about a particular stress σ_0 the energy can be written as

$$Q(\sigma) = Q(\sigma_0) + (dQ/d\sigma)(\sigma - \sigma_0) \quad (25)$$

One now assumes that steady state creep is an activated process, and the rate of change of the activation energy with stress ($dQ/d\sigma$) is a constant B . The steady state creep rate must then follow a creep equation of the type

$$\text{Creep rate } K = A \exp\{-Q/kT\} \exp\{B\sigma/kT\} \quad (26)$$

(b) Creep Data for Fine-Grained As-Extruded Alloys

Steady state creep rates for two fine-grained, as-extruded S.A.P.-type alloys have been obtained. These alloys, MD 2100 and M

257, in the as-extruded condition have needle-like grains, about 5μ in diameter, but many microns long. Both have an average dispersed particle spacing of approximately 0.5μ . The M 257 is a commercial grade of aluminum powder metallurgy product.

The alloy MD 2100 is the only one for which steady state creep rates were determined in both the as-extruded and the recrystallized, coarse-grained condition. As mentioned above the rate for the alloy in the recrystallized conditions was so low that it could not be measured. The creep rate of the alloy in the as-extruded condition, on the other hand, was appreciable. Such a slower creep rate for an alloy

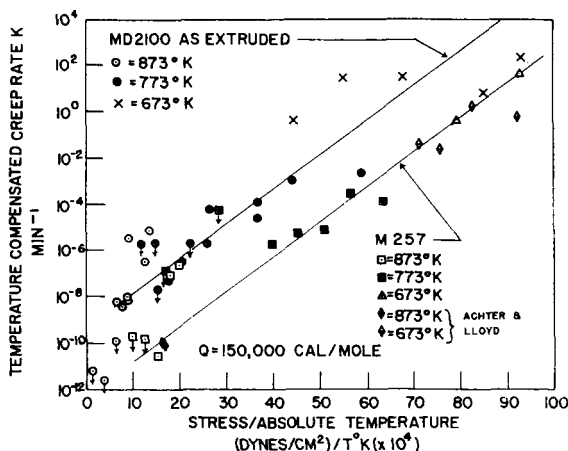


Fig. 11. The logarithm of the temperature-compensated steady state creep rates of the fine-grained MD 2100 and M 257 Al-Al₂O₃ S.A.P.-type alloys are plotted vs the stress divided by temperature.

in the recrystallized condition can be expected only in alloy systems such as the aluminum-aluminum oxide system, in which the second phase is stable enough so that the dispersion does not coarsen even during the drastic mechanical and thermal treatment necessary for recrystallization.

The steady state creep rates of the two fine-grained alloys, when measured at a single temperature, followed an equation of the type

$$\text{Creep rate, } K = A \exp\{B\sigma/kT\} \quad (27)$$

where A and B are constants. From eq. (27) the data taken at

several temperatures were compensated to a single test temperature by eliminating temperature as a variable and deriving a temperature-compensated steady state creep rate K^* , where

$$K^* = K(\exp\{-Q/R\theta\})/(\exp\{-Q/RT\}) \quad (28)$$

In Figure 11, the logarithm of the steady state creep rate of both fine-grained alloys compensated to 500°C was plotted versus stress divided by temperature. The value of the activation energy Q which best fits this relationship was 150,000 cal/mole.

These data are in agreement with the qualitative theory for steady state creep of fine-grained dispersion-strengthened alloys, where the rate-controlling process for creep is the nucleation of dislocations from grain boundaries.

VI. OTHER STRENGTH PROPERTIES

In the preceding sections several of the strength properties of dispersion-strengthened alloys (i.e., yielding and steady state creep) have been handled in a rather fundamental way with a fair degree of success. There are however other properties which constitute the mechanical strength of a dispersion-strengthened alloy. These include fracture mode, stress rupture, ductility, transient creep behavior, work hardening, and recovery.

These areas of strength, which have not yet been covered in a fundamental way for dispersion-strengthened alloys, are difficult to treat fundamentally. Unlike yielding and steady state creep behavior, they cannot be considered in terms of unique dislocation or metallurgical structure. Rather, one has to determine the changes in microstructure and dislocation arrays as a function of strain, strain rate, stress, and temperature.

There are directions which may prove fruitful in these studies. Stress rupture, ductility, work hardening, and recovery are properties which are more or less interdependent. If one treats the rate of crack propagation, the rate of recovery, and the rate of work hardening as independent processes, then it should be possible to evaluate composite properties like stress to rupture and ductility. It is this line of approach which should be used in further studies of the strengthening effects of a dispersed phase.

In conclusion it should be pointed out that a mechanism or model proposed to explain a particular mechanical property of a metal can

only be expected to explain the behavior of those alloy systems to which the fundamental assumptions of the model apply. In the theoretical work presented here, it has always been assumed that dislocations in the structure are interacting with a particular dispersion morphology. If the dispersion morphology is changing during the testing or application of any dispersion-strengthened alloy, one cannot expect these models to predict their behavior unless the change in morphology can be delineated. This is particularly important when one is considering elevated temperature strength.

VII. CONCLUSIONS

1. A dislocation model is proposed for yielding of dispersion-strengthened alloys. The criterion for yielding is the fracture of the dispersed second phase particles due to an array of piled-up dislocation loops.

2. Calculations based upon this dislocation model for yielding indicate that the yield strength of a dispersion-strengthened alloy is proportional both to the reciprocal square root of the dispersed particle spacing and to the product of the square roots of the shear moduli of the dispersed phase and the matrix metal.

3. Experimental data for the yielding behavior of several types of dispersion-strengthened alloys as a function of dispersion spacing, temperature, and shear modulus of the dispersed phase are in agreement with the calculation based on the dislocation model for yielding.

4. Dislocation models, proposed by Ansell and Weertman to account for the steady state creep behavior of dispersion-strengthened alloys, are reviewed. The rate-controlling processes for steady state creep used in these models are dislocation climb for alloys in which Frank-Read dislocation sources are operative in the alloy and nucleation of dislocations from grain boundaries for alloys in which the usual Frank-Read dislocation sources are not active.

5. Steady state creep data for several large-grained aluminum S.A.P.-type alloys, in which active Frank-Read dislocation sources are assumed to be present, are in agreement with the stress, temperature, and dispersion spacing dependence as predicted by the dislocation theory for creep based upon dislocation climb. The absolute value of the creep rate is, however, several orders of magnitude lower than that predicted by the theory. This indicates that the density of

dislocation sources in a dispersion-strengthened alloy is much lower than in a single phase metal.

6. Steady state creep data for several fine-grained aluminum S.A.P.-type alloys, in which the usual Frank-Read dislocation sources are not active, are in agreement with the dislocation theory presented in which the rate-controlling process for steady state creep is the nucleation of dislocations from grain boundaries.

7. Although several of the strength properties of dispersion-strengthened alloys (namely, yielding and steady state creep behavior) appear now to be explained on a fundamental basis, there are several other strength properties—ductility, fracture, stress to rupture, and work hardening—which are not yet well understood.

The support of the investigations upon which this paper is based, by the National Aeronautics and Space Administration, is gratefully acknowledged.

References

1. Goetzel, C. G., *J. Metals*, **11**, 189, 276 (1959).
2. Geisler, A. H., *Phase Transformations in Solids*, Wiley, New York, 1951.
3. Gensamer, M., E. B. Pearsall, W. S. Pellini, and J. R. Low, Jr., *Trans. Am. Soc. Metals*, **30**, 983 (1942).
4. Roberts, C. S., R. C. Carruthers, and B. C. Averbach, *Trans. Am. Soc. Metals*, **44**, 1150 (1952).
5. Orowan, E., *Symposium on Internal Stresses in Metals and Alloys*, Inst. of Metals, London 1948.
6. Orowan, E., *Dislocations in Metals*, Am. Inst. of Mining, Met. and Petrol. Eng., New York (1954).
7. Fisher, J. C., E. W. Hart, and R. H. Pry, *Acta Met.*, **1**, 336 (1953).
8. Cottrell, A. H., *Dislocations and Plastic Flow in Crystals*, Oxford Univ. Press, New York, 1953, p. 11.
9. Petch, N. J., *J. Iron Steel Inst. (London)*, **174**, 25 (1953).
10. Lenel, F. V., G. S. Ansell, and E. C. Nelson, *Trans. AIME*, **209**, 117 (1957).
11. Lenel, F. V., A. B. Backensto, Jr., and M. C. Rose, *Trans. AIME*, **209**, 124 (1957).
12. Lyle, J. P., Jr., *Metal Progr.*, **62**, No. 6, 109 (1952).
13. Dew-Hughes, D., and W. D. Robertson, *Acta Met.*, to be published.
14. Lenel, F. V., G. S. Ansell, and R. Bosch, to be published.
15. Sutton, P. M., *Phys. Rev.*, **19**, 816 (1953).
16. Stavrolakis, J. A., and F. H. Norton, *J. Am. Ceram. Soc.*, **33**, 263 (1950).
17. Grant, N. J., and O. Preston, *Trans. AIME*, **309**, 349 (1957).
18. Barrett, C. S., *Acta Met.*, **1**, 2 (1953).
19. Ansell, G. S., and Weertman, J., *Trans. AIME*, **215**, 838 (1959).
20. Lenel, F. V., in R. F. Hehemann and G. M. Ault, eds., *High Temperature Materials*, Wiley, New York, 1959, p. 321.
21. Weertman, J., *J. Appl. Phys.*, **28**, 362 (1957).

22. Weertman, J., *J. Appl. Phys.*, **28**, 1185 (1957).
23. Schoeck, S., *Creep and Recovery*, Am. Soc. for Metals, Cleveland, 1957, p. 199.
24. Friedel, J., *Phil. Mag.*, **46**, 1169 (1955).
25. Weertman, J., *J. Appl. Phys.*, **26**, 1213 (1955).
26. Ansell, G. S., *Trans. AIME*, **215**, 294 (1959).

Discussion

L. J. Bonis (*Massachusetts Inst. of Technol.*): The theoretical explanation of dispersion strengthening and calculations look extremely interesting and promising. There remains, however, the applicability of this theory for other similar systems outside of the Al-Al₂O₃ range.

We applied the approach described in the paper on two different internally oxidized systems. A Ni-1.25 wt-% Al alloy internally oxidized at 750°C (5.58 vol-% Al₂O₃), mean free path 0.8 β (No. 68 in Discussion Table I); a Ni-2.27 wt-% Al alloy internally oxidized at 750°C (10.44 vol-% Al₂O₃), mean free path 0.6 μ (69 in Discussion Table I), and a Cu-0.77 wt-% Al alloy internally oxidized at 950°C (3.5 vol-% Al₂O₃), mean free path 0.31 μ (B-33 in table). The results are shown in Discussion Table I.

DISCUSSION TABLE I

Temperature Compensated Minimum Creep Rate (T.C.M.C.R.) of Ni-1.25 Al (68), Ni-2.27 Al(69), Cu-0.77 Al(B33)

Alloy No.	Temperature		Stress		MCR min ⁻¹	T.C.M.C.R. ^a
	°F	°K	psi	dynes/cm ²		
68	1300	978	15000	1.03 × 10 ⁹	8.84 × 10 ⁻⁵	8.84 × 10 ⁻⁵
	1500	1089	8000	5.5 × 10 ⁸	7.67 × 10 ⁻⁶	3.28 × 10 ⁻⁷
	1800	1255	5000	3.44 × 10 ⁸	1.18 × 10 ⁻⁴	4.8167 × 10 ⁻⁸
69	1800	1225	5000	3.44 × 10 ⁸	1.15 × 10 ⁻⁶	4.705 × 10 ⁻¹⁰
68	1500	1089	12000	8.27 × 10 ⁸	5.0 × 10 ⁻⁷	1.39 × 10 ⁻⁸
69	1800	1255	6000	4.137 × 10 ⁸	3.07 × 10 ⁻⁵	1.253 × 10 ⁻⁷
68	1500	1089	8000	5.5 × 10 ⁸	7.16 × 10 ⁻⁶	1.99 × 10 ⁻⁷
68	1500	1089	9000	6.2 × 10 ⁸	2.88 × 10 ⁻⁵	8.0 × 10 ⁻⁷
68	1500	1089	10000	6.89 × 10 ⁸	1.6 × 10 ⁻⁴	4.5 × 10 ⁻⁶
68	1300	978	11000	7.58 × 10 ⁸	1.28 × 10 ⁻⁶	1.28 × 10 ⁻⁶
68	1300	978	13000	8.96 × 10 ⁸	8.48 × 10 ⁻⁵	8.48 × 10 ⁻⁵
68	1300	978	10000	6.89 × 10 ⁸	4.75 × 10 ⁻⁷	4.75 × 10 ⁻⁷
B-33	845	723	40000	2.76 × 10 ⁹	1.4 × 10 ⁻³	1.4 × 10 ⁻³
	845	723	35000	2.41 × 10 ⁹	8.3 × 10 ⁻⁵	8.3 × 10 ⁻⁵
	1205	923	21000	1.48 × 10 ⁹	1.0 × 10 ⁻⁴	4.1 × 10 ⁻⁷
	1565	1123	12000	8.27 × 10 ⁸	8.3 × 10 ⁻³	3.07 × 10 ⁻⁷
	1565	1123	14000	9.65 × 10 ⁸	1.5 × 10 ⁻¹	5.5 × 10 ⁻⁶
	1565	1123	8000	5.5 × 10 ⁸	5.8 × 10 ⁻⁵	2.1 × 10 ⁻⁹
	1565	1123	10000	6.89 × 10 ⁸	2.5 × 10 ⁻⁴	9.5 × 10 ⁻⁹

^a Data compensated to reference temperature assuming eq. (24) is applicable.

G. S. Ansell: The minimum creep rate data referred to by Mr. Bonis for the Ni-Al₂O₃ and Cu-Al₂O₃ dispersion-strengthened alloys are quite interesting. We have presented the steady-state creep data for the Al-Al₂O₃ system only because these alloys have an extremely stable structure at elevated temperatures. The theoretical treatment presented to explain the steady-state creep behavior of dispersion-strengthened alloys should of course be applicable to any other alloy with both a suitably dispersed second-phase and a similar structural stability at high temperatures.

In view of this, it is important now to compare the steady-state creep data presented by Mr. Bonis in terms of the creep theory. First, one must consider two factors. (1) Is the second-phase suitably dispersed? (2) Are the structures of these alloys stable at the testing temperature? It is reasonable to assume that at test temperature these are stable systems with a suitably dispersed second-phase. Now one can compare the data with the creep theory. The data were taken in a stress range below and above that where $n\sigma b^3/kT = 1$. For the lower stresses eq. (21) should therefore be applicable, i.e., the creep rate should be proportional to the fourth power of the applied stress, while for the higher stresses, eq. (23) should apply, where rate is an exponential function of the applied stress. A plot of the data at each temperature shows that the theory reasonably describes the creep behavior. Because of this change in stress dependence of the creep data the data presented cannot be compensated to a single test temperature using as a basis only eq. (24).

It is interesting to note that we have been unable to obtain minimum or steady-state creep data for the Al-Al₂O₃ alloys in the stress range where eq. (23) is applicable due to rapid specimen fracture. The data provided by Mr. Bonis extends the stress range over which the creep theory may be verified with experimental data.

H. Bückle (*Office National d'Etudes et de Recherches Aeronautiques, France*): It is worthwhile noting that the strengthening effect of dispersed phases (heterogeneous alloys) finds to some extent an analogy in the case of entirely homogeneous phases which have undergone heavy cold work or have extremely small grain sizes. Even in the case of pure metals, the hardness values show a very considerable increase with decreasing grain size below about 1 μ . With further decrease in grain size, the microhardness number tends toward a saturation value equal to 3 or 4 times that of a single crystal, this level being approached with grain diameters of less than 0.1 μ . A limiting value of the same order of magnitude (factor 3.7) has been postulated by Tabor for heavily cold-worked metals, and this again could be confirmed by microhardness studies. Similar results were achieved by testing heterogeneous samples consisting of a matrix with precipitates. It should be noted that in the case of very fine precipitates, the hardness variation seems to be independent of the nature of the precipitate, depending only on their spacing, so that dispersed pores of less than 0.1 μ diam may have a notable hardening effect. With further decreasing spacing of the fine precipitates, the microhardness values seem to approach a limiting level as described above. These phenomena can be explained on a common basis, if the segregates, precipitates, local stress concentrations, grain boundaries, sub-grains, and the like are considered as more or less equivalent "dislocation traps," forming a network of meshes which have the

diameter of the potential mean free path of the dislocations. To simplify the discussions, we suggested calling these undisturbed volume units "coherent regions" (H. Bückle, "L'essai de microdureté et ses applications," Publications Scientifiques et Techniques du Ministère de l'Air, Paris, 1960). Clearly, the saturation value must be reached if their diameter reaches the dimensions of a dislocation, i.e., 10^{-4} - 10^{-6} cm. The specimen consists then entirely of "disturbed matter" and therefore must behave as a quasi-amorphous sample where crystalline gliding is no longer possible. Likewise, in the case of dispersed phases, a maximum strengthening should occur if both the dispersed phases as well as their spacing approach the above-mentioned dimensions. So, for example, we should reasonably expect that the curves shown by Drs. Lenel and Ansell and representing some mechanical data as a function of $1/\sqrt{\lambda}$ should cease to be linear and should tend toward some saturation value if the abscissa values are in excess of about $3 \mu^{-1/2}$ (i.e., $\lambda < 0.1 \mu$).

It should be clearly understood that I do not suggest transposing simply the microhardness results to the problem of creep stress and related stress problems. One must also keep in mind the factor of the thermal stability; in fact, very fine-grained or heavy cold-worked pure metals recrystallize easily, dispersed fine pores can coalesce and grow, etc. Nevertheless, I think that the general description in terms of coherent regions, admittedly somewhat rough, lends itself to a quite useful tentative approach as the basis of comparative studies.

D. H. Feisel (*Westinghouse Research Labs.*): In work I am doing with nickel-base alloys dispersion hardened by alumina, I find that the proportional limit in compression is always higher than that in tension, and in some cases there is a factor of two involved. In creep tests, for a given set of conditions, the creep rate in compression has been found to be much lower than that in tension. Would the authors care to comment on these observations?

G. S. Ansell: The authors have no explanation for this behavior.

R. Steinitz (*General Telephone and Electronics Labs.*): What is the influence of porosity on the strengthening effect of a dispersed phase? Does porosity lower the strength of such a material in the same way and by the same amount as it would do in the pure matrix metal, or do pores more or less destroy the whole effect of the dispersed phase, and make the material behave like the pure metal? I am considering a porosity of about 10-15% with small, finely distributed pores.

G. S. Ansell: If the pores have a strong, adherent coating such as an oxide, they act just as the dispersed phase. If, on the other hand, the pore surface is clean, then the pores have three effects. The first, and most important effect, is that the free surface of the pore acts as a sink for dislocations. If the pores and the dispersed-phase particles are associated then this prevents the dispersed phase from acting as an effective barrier to dislocation motion. If the pores are separate from the dispersed-phase particles then the relative morphology of pore distribution to second phase particles becomes important. In an amount dependent upon this relative distribution, the effectiveness of the dispersed particles in increasing the yield strength and reducing the steady state creep rate is lowered. The second effect is that dislocations will extend from pore to pore. To move dislocations in the matrix, stress must be supplied either to make these dislocation segments break away from the pores or to operate as a Frank-Read source. This strengthening

effect would affect the yielding behavior and would require a mean interpore spacing which is much less than the dispersed-particle spacing. The third effect is that the pores could act as sources for dislocations, just as in the case of grain boundaries in the as-extruded S.A.P. alloys. In this case, the steady state creep rate of a large grained material would be much faster with pores than without pores.

It is realized that these are quite generalized statements. In considering the effect of pores in the structure a more specific answer is not possible unless the pore shape and distribution, matrix metal, and dispersed-phase shape and distribution are specified so that the relative effect of each of these may be calculated.